

LAL 01-24
 LBNL-47757
 May 2001

CP Violation and the Absence of Second Class Currents in Charmless B Decays

Sandrine Laplace

Laboratoire de l'Accélérateur Linéaire, IN2P3-CNRS et Université Paris-Sud
 BP 34, F-91898 Orsay Cedex, France
 E-mail: laplace@lal.in2p3.fr

Vasia Shelkov

Lawrence Berkeley National Laboratory, 1, Cyclotron Road, Berkeley, CA 94720, USA
 E-mail: VG.Shelkov@lbl.gov

The absence of second class currents together with the assumption of factorization for non-leptonic B decays provides new constraints on CP observables in decay $B \rightarrow a_0(980) \pi \pi$. The kinematics of this decay does not allow interference between the oppositely charged resonances in the Dalitz plot as in $B^0 \rightarrow D^0 \pi^0 \pi^0$. Nonetheless, the $B \rightarrow a_0$ two-body time-dependent isospin analysis leads to a more robust extraction of the angle than in the $B \rightarrow \pi^0 \pi^0 \pi^0$ isospin-pentagon analysis. The absence of second class currents might lead to enhanced direct CP violation and/or allows for a test of some assumptions made in the analysis in other decays like $B \rightarrow a_0 \pi^0$, $B \rightarrow b_1(1235) \pi^0$, $B \rightarrow a_0 a_0$, $B \rightarrow \pi^0 \pi^0 \pi^0$ and $B \rightarrow b_1 a_0$.

1 Introduction

The usefulness of the $B \rightarrow a_0$ decay for measuring the angle of the unitarity triangle by a time-dependent three-body Dalitz plot¹ or a two-body isospin^{2,3} analysis has been emphasized recently by Dighe and Kinn⁴. It thus joins the list of channels like $B \rightarrow \pi^0 \pi^0 \pi^0$ and $B \rightarrow \pi^0 \pi^0 \eta$ allowing the extraction of β .

These latter channels suffer from serious experimental limitations. The $B \rightarrow \pi^0 \pi^0 \pi^0$ decays have low branching fractions^{5,6} and measuring the $\pi^0 \pi^0 \pi^0$ final state is an experimental challenge. The branching ratio of the $B \rightarrow \pi^0 \eta$ decay is larger^{5,6} but this channel suffers from combinatorial background due to the presence of a $\pi^0 \eta$ and contamination from higher excitations⁷, which complicate the time-dependent Dalitz-plot analysis. The $B \rightarrow a_0$ decay has some advantages from the experimental point of view, as pointed out by Dighe and Kinn⁴, since it is easier to reconstruct the a_0 than the $\pi^0 \eta$ (due the higher energies of the final state photons) and since the width of the a_0 is narrower (around 60 MeV⁸) than the width of the $\pi^0 \eta$ (150 MeV⁸). These properties help to reduce the combinatorial background, and should thus provide a cleaner signal sample than for the $B \rightarrow \pi^0 \eta$ mode.

However, the interference pattern, which is effective in $B \rightarrow \pi^0 \eta$, is kinematically suppressed in $B \rightarrow a_0$. There is simply no overlap between the $B^0 \rightarrow a_0^+ \pi^0$ ($a_0^+ \rightarrow \pi^0 \eta$) and $B^0 \rightarrow a_0^+ \pi^0$ ($a_0^+ \rightarrow \pi^0 \eta$) bands in the

Dalitz plot, which usually provides the main source of interference.

Focusing on the decays $B \rightarrow a_0$ and $B \rightarrow a_0$, we show in this paper that their analysis as two-body decays, because of the absence of second class currents^a, leads to a more robust^b determination of the angle β , than the original isospin-pentagon analysis proposed by Lipkin, Nir, Quinn and Snyder³ for $B \rightarrow \pi^0 \eta$ and applied to $B \rightarrow a_0$ by Dighe and Kinn⁴.

The time-dependent two-body $B \rightarrow a_0$ analyses proceed through seven to nine-parameters depending on whether or not the charged modes are considered. When statistics is limited, simpler four-parameters can be performed for $B \rightarrow a_0$ decays by using one theoretical prediction of an amplitude (or a ratio of two of them).

Moreover, as advocated in Section 3.6, the elimination of leading tree contribution due to the suppression of second class currents may give rise to enhanced direct CP violation in the decay $B \rightarrow a_0$, as well as $B \rightarrow b_1$ and $B \rightarrow \pi^0 \eta$.

^a This was first pointed out to us by J. Charles in a private communication.

^b The analysis is more robust in the sense that there are either more degrees of freedom or less unknowns in the extracting, which makes the more stable.

2 The absence of Second Class Currents in some Non-Leptonic B^- Decays

In tree diagrams contributing to non-leptonic B^- decays, part of the hadronic system is produced via coupling of the virtual W^- to the quark current. Charmless final states with zero net strangeness proceed via the $W^- + \bar{u}d$ coupling, with rates proportional to the CKM matrix element y_{ud} .

Assuming factorization, the color singlet pair of quarks hadronizes independently of the rest of the B^- decay. This implies that there is no re-scattering (or final state interaction) between the hadrons coming from the W^- and the other hadrons of the final state. Under this assumption, the production of hadrons resulting from the coupling of quarks to the virtual W^- abide by the same rules as semi-leptonic decays. We recall some of the relevant properties in the following.

The vector part of the weak current $u^- (1 \quad 5) d$ has even G-parity, whereas the axial part has odd G-parity. It follows that a virtual W^+ decaying to ud produces states with an even G-parity and natural spin-parity ($0^+ ; 1^- ; \dots$), or with an odd G-parity and unnatural spin-parity ($0^- ; 1^+ ; \dots$). Decays with opposite combinations of G- and spin-parity are called second class currents, and are forbidden in the Standard Model up to isospin violations. This is the case for the a_0^- which has $G = -1$ and $J^P = 0^+$, and the b_1^- which has $G = +1$ and $J^P = 1^+$. Experimental limits on second class currents are obtained, e.g., from the measurement of $a_0^- + b_1^-$ branching fraction for which the present limit reads 1.4×10^{-4} at 95% CL⁸.

States with $J^P = 0^+$ are also forbidden by the conservation of the vector current, independently of their G-parity, up to isospin violating corrections. Therefore the $W^- + a_0^-$ decay is doubly-suppressed.

Contributions from annihilation and exchange diagrams are neglected since they are expected to be suppressed by helicity conservation (giving a term $/m_{ud}^2 = m_B^2$ in the amplitude expression) and by the quantity $f_B = m_B$, where f_B is the decay constant of the B^- .

Thus, assuming factorization, the absence of second class currents leads to the suppression of tree diagrams in which the a_0^- (b_1^-) and the virtual W^- have the same charge.

Experimental tests of the factorization assumption for the decays treated in this paper are proposed in Sec. 3.1.

3 Extracting from $B^- + a_0^-$ and $B^- + b_1^-$ Decays

This section aims at showing the consequences of the absence of second class currents in the extraction of a_0^- in

the $B^- + a_0^-$ and $B^- + b_1^-$ decays. The phase-space analyses of $B^- + a_0^-$ and $B^- + b_1^-$ are not as powerful as for $B^- + a_0^-$, since the interferences between the different resonances are weak (see Sec. 3.2 and 3.3).

The emphasis is put on the $B^- + a_0^-$ time-dependent two-body analysis, which can be performed separately for $B^- + a_0^-$ and $B^- + b_1^-$. In effect, one could use both modes in a combined fit, hence reducing the number of linear solutions for the angle (cf Sec. 3.5).

On the one hand, the branching ratio of $B^- + a_0^-$ is expected to be formally enhanced with respect to $B^- + b_1^-$. On the other hand, decays involving a charged ($B^- + a_0^0$) require the reconstruction of an additional π^0 . Finally, in contrast to $B^- + a_0^-$, the time-dependence of $B^- + a_0^0$ is measurable due to the charged products of the $\pi^0 + \pi^+$.

3.1 Tree and Penguin Contributions and Consequences of the Absence of Second Class Currents

In processes involving uud non-spectator quarks, the decay amplitude can be expressed in terms of the tree (T) and u -, c - and t -penguin (P^u , P^c , P^t) contributions (where the CKM matrix elements have been explicitly factorized out):

$$A(uud) = V_{tb}V_{td}P^t + V_{cb}V_{cd}P^c + V_{ub}V_{ud}(T + P^u) ; \\ = V_{tb}V_{td}(P^t - P^c) + V_{ub}V_{ud}(T + P^u - P^c) ; \quad (1)$$

The second line is obtained by using the unitarity relation $V_{ub}V_{ud} + V_{cb}V_{cd} + V_{tb}V_{td} = 0$. The amplitude is thus the sum of two terms depending on the weak phases

(from V_{td}) and (from V_{ub}). We will neglect the contributions from P^u and P^c and propose a test of this assumption later in this section. Therefore, the remaining t -penguin provides, whereas is only invoked by the tree amplitude. We will denote these two contributions T and P in the following, where P is restricted to the t -penguin contribution only.

The $B^- + a_0^i$ ($i = 0, +, -$) decay amplitudes A^{ij} can thus be expressed in terms of tree (T^{ij}) and penguin (P^{ij}) contributions and the weak phase θ . For example, the amplitudes for the $B^- + a_0^-$ decay read:

$$A(B^- + a_0^+) = A^+ = e^{i\theta} T^+ + P^+ ; \quad (2)$$

$$A(B^- + a_0^-) = A^- = e^{i\theta} T^- + P^- ; \quad (3)$$

$$A(B^- + a_0^0) = A^{00} = e^{i\theta} T^{00} + P^{00} ; \quad (4)$$

$$A(\bar{B}^0 + a_0^+) = \bar{A}^+ = e^{+i\theta} T^+ + P^+ ; \quad (5)$$

$$A(\bar{B}^0 + a_0^-) = \bar{A}^- = e^{+i\theta} T^- + P^- ; \quad (6)$$

$$A(\bar{B}^0 + a_0^0) = \bar{A}^{00} = e^{+i\theta} T^{00} + P^{00} ; \quad (7)$$

where the $q\bar{q}$ mixing parameter⁹ has been absorbed in the A amplitudes, leading to the explicit presence of the angle θ . The T^+ amplitude comes from the

W^+ ! a_0^+ transition, and is suppressed as a Second Class Current Forbidden Tree (SCCFT). Therefore, the $A(B^0 ! a_0^+ =)$ and $A(\overline{B}^0 ! a_0^+ = +)$ amplitudes are pure penguin transitions, and cannot display direct CP violation:

$$A(B^0 ! a_0^+ =) = A^+ = P^+ ; \quad (8)$$

$$A(\overline{B}^0 ! a_0^+ = +) = \overline{A}^+ = P^+ ; \quad (9)$$

and therefore

$$A(B^0 ! a_0^+ =) = A(\overline{B}^0 ! a_0^+ = +) ; \quad (10)$$

The question arises what could break equality (10). Since electroweak penguins exhibit the same weak phase as the gluonic penguins, they would not modify it, but would break isospin relations used in the analysis. The u or c-loop penguins have both different weak and strong phases than the remaining penguin P^+ , they thus fail the conditions for producing direct CP violation. Therefore, if their contribution is not negligible, they would break equality (10). So would a failure of factorization, since the final state corresponding to the forbidden tree T^+ transition would be produced by re-scattering from the other tree T^+ , thus providing the needed phases for direct CP violation.

Therefore, the equality (10) is primarily a test of the factorization hypothesis and of the validity of neglecting u and c penguin contributions.

3.2 The $B ! a_0$ Three-Body Analysis a la

Dighe and Klem⁴ have proposed to extract a_0 from the $B ! a_0$ decay using both two-body isospin and three-body Dalitz plot analyses.

The Dalitz-plot analysis fails because of the small interference between the oppositely-charged a_0 , as shown in Fig.1. Since most of the interference occurs when the two resonance bands intersect, the regions covering three times the width (called "3 interference region") are indicated for the a_0 and ρ resonances. Kinematic boundaries for $B^0 ! a_0^+ +$ and $B^+ ! a_0^+ +$ are also drawn. The shape of the boundary in the left-hand bottom corner of the $B ! a_0$ Dalitz plot is determined by the mass, which limits the available phase-space. In contrast to in the $B^+ ! a_0^+ +$ decay, the a_0 mass and width are too small to allow strong interferences within the kinematic limits of the Dalitz plot.

Interferences can still occur far away from the 3 interference region, but they are less than 1% in the case of $B ! a_0$ and occur in the badly-known tails of the a_0 resonance.

Therefore, the Dalitz-plot analysis for $B ! a_0$ is not of interest.

⁴ cf Sec. 3.3 for the description of a method on how to compute the strength of the interferences.

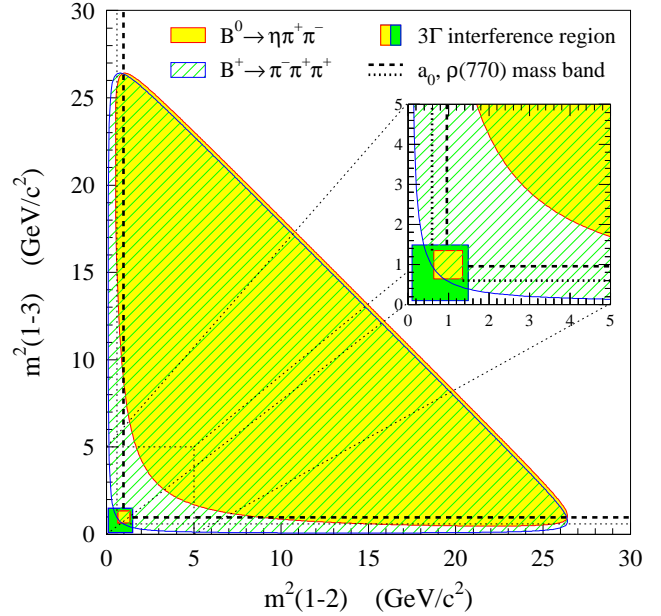


Figure 1: Dalitz plot kinematic boundaries for the $B^0 ! a_0^+$ and $B^+ ! a_0^+$ decays. The dashed (dotted) line shows the $a_0 (\rho)$ mass band. The 3 Γ interference regions for the a_0 (light shade) and ρ (dark shade) resonances are also drawn, the region for the a_0 laying outside the allowed boundary of the $B ! a_0$ Dalitz plot.

3.3 The $B ! a_0$ Four-Body Analysis

The modes $B^0 ! a_0^+ +$, $B^0 ! a_0^+ +$ and $B^0 ! a_0^0 +$ decay into the common four-body final state $+ + +$. If interference between a_0 's and ρ 's is strong enough, one could perform a similar time and phase-space dependent analysis as for $B ! a_0$.

To quantify the strength of the interferences, the following parameter⁷ can be evaluated:

$$= \sum_{i=1}^{X^3} f_i^2 \cdot \sum_{j=1}^{X^3} f_j^2 - 1 ; \quad (11)$$

where $f_1 = f(a_0^+) f(\rho) \cos \theta$, $f_2 = f(a_0^0) f(\rho) \cos \theta$, and $f_3 = f(a_0^0) f(\rho) \cos \theta$ are the products of the a_0 and ρ Breit-Wigner parameters, taking into account the distribution of the helicity angle (θ defined as the angle between the decay axis in the rest frame and the direction of the ρ in the laboratory frame). Using simple relativistic Breit-Wigner parameterizations for the a_0 and the a_0 resonances^d, the parameter distribution is computed using $B ! a_0$ Monte Carlo events. The mean value of j is equal to 10%, corresponding to roughly half of what

^d The a_0 mass parameterization is complicated by the $K\bar{K}$ -production threshold⁸, and is not well-known. Using a simple Breit-Wigner is a rough approximation.

is observed in $B^0 \rightarrow a_0^0$. Therefore the $B^0 \rightarrow a_0^0$ decay only provide poor interference.

Additional complication of having to reconstruct an extra neutral particle makes this channel less accessible than $B^0 \rightarrow a_0^0$. Nevertheless, the time and phase-space dependent analysis of the $B^0 \rightarrow a_0^0$ decay provides an independent and complementary way of measuring the angle without any ambiguities.

3.4 The $B^0 \rightarrow a_0^0$ Two-Body Time-Dependent Analyses

Since the $B^0 \rightarrow a_0^0$ three-body final state does not exhibit interference in the Dalitz plot, one is led to a two-body analysis, i.e. where $B^0 \rightarrow a_0^0$ and $B^0 \rightarrow a_0^+$ decays are considered as two-body final states. The analysis can be applied to $B^0 \rightarrow a_0^+$ as well.

The time-dependent amplitudes for the two-body decays $B^0(t) \rightarrow a_0^+$ and $B^0(t) \rightarrow a_0^0$ (as well as for the CP-eigenstate $B^0 \rightarrow a_0^0$) read:

$$A(B^0(t) \rightarrow a_0^+) / e^{-\frac{1}{2}t^2} \stackrel{h}{=} \cos\left(\frac{m}{2}t\right) A^+ + i \sin\left(\frac{m}{2}t\right) \bar{A}^+ \quad (12)$$

$$A(B^0(t) \rightarrow a_0^0) = e^{-\frac{1}{2}t^2} \stackrel{h}{=} \cos\left(\frac{m}{2}t\right) A^0 + i \sin\left(\frac{m}{2}t\right) \bar{A}^0; \quad (13)$$

where the cosine and sine terms describe the $B^0 \bar{B}^0$ flavor mixing, and t is the difference of decay time between the two mesons produced at the $(4S)$ resonance in an asymmetric B factory. The A^+ , A^0 , \bar{A}^+ and \bar{A}^0 amplitudes are defined in Eqs. (2)–(9).

The time-dependent decay rate is obtained by squaring Eqs. (12) and (13), which leads to terms proportional to $\sin^2(m t/2)$, $\cos^2(m t/2)$ and $\sin(m t)$:

$$(B^0(t) \rightarrow a_0^0) / e^{-\frac{1}{2}t^2} \stackrel{h}{=} A_1 \sin^2\left(\frac{m}{2}t\right) + A_2 \cos^2\left(\frac{m}{2}t\right) + A_3 \sin(m t) / e^{-\frac{1}{2}t^2} A_1^0 + A_2^0 \cos(m t) + A_3^0 \sin(m t); \quad (14)$$

where the $A_{1,2,3}$, $A_{1,2}^0$ terms are combinations of the a_0^0 amplitudes.

Therefore, each time-dependent $B^0 \rightarrow a_0^0$ ($+$), $B^0 \rightarrow a_0^+$ ($+$) and $B^0 \rightarrow a_0^0$ (0) measurement provides three observables: A_1^0 , A_2^0 and A_3^0 .

The measurement of the branching ratios for charged B decays $B^0 \rightarrow a_0^+$ and/or for the neutral final state $B^0 \rightarrow a_0^0$ (0) each provides one observable. Using isospin invariance^{2,3,9}, one can link the penguin and tree contributions from neutral and charged B decays, which

provides the missing pieces for the extraction of :

$$P \frac{1}{2} T^{+0} + T^{0+} = T^+ + T^+ + 2T^{00}; \quad (15)$$

$$P^{00} = \frac{1}{2} (P^+ + P^-); \quad (16)$$

$$P^{+0} = \frac{1}{P^+} (P^+ - P^-); \quad (17)$$

$$P^{0+} = \frac{1}{P^-} (P^+ - P^-); \quad (18)$$

Table 1 gives a comparison of the number of observables and unknowns for $B^0 \rightarrow a_0^0$, $B^0 \rightarrow a_0^+$, $B^0 \rightarrow a_0^0$ and $B^0 \rightarrow a_0^+$ analyses. Three analyses steps are described: in the upper part of the table, only charged final states of neutral B decays are used. In the middle part, neutral final states of neutral B decays are added. In the lower part, both neutral and charged B decays are taken into account. Available isospin relations are indicated at each analyses stage.

The leading contribution to $B^0 \rightarrow a_0^0$, the T^0 tree, is suppressed by SC CFT. One of the two contributions to the color-suppressed T^{00} amplitude is removed by the same SC CFT argument^e, but the other contribution remains. The leading contribution to the T^{+0} amplitude is removed by SC CFT, but a color-suppressed contribution remains.

The number of unknowns is given by the sum of tree and penguin complex amplitudes involved at each analyses stage, plus the angle. One unphysical overall phase and one irrelevant overall normalization constant are subtracted from the total.

The number of observables available from a time dependent measurement is three (cf Eq. (14)), and one for the time integrated measurement. The overall normalization is subtracted from the sum of observables.

Using only the charged final states of the neutral B decays does not provide enough observables to constrain in any of the four analyses considered. Nevertheless, using a single theoretical prediction for an amplitude (or a ratio of amplitudes) in four-parameter $B^0 \rightarrow a_0^0$ and two-parameter $B^0 \rightarrow a_0^+$ would be enough to extract the value of α . Such a model-dependent approach can be performed with low statistics.

Adding the neutral final states does not further constrain the α s, neither for $B^0 \rightarrow a_0^0$, nor for $B^0 \rightarrow a_0^+$, $B^0 \rightarrow a_0^0$. In contrast, the $B^0 \rightarrow a_0^0$ analysis does improve, since time-dependence is observable and SC CFT holds, though the t is only barely constrained (seven observables vs seven unknowns).

Adding charged B decays in the analyses allows all four α s to converge, but with different robustness:

^e This is because this contribution to the T^{00} amplitude is the Fierz-transform of T^+ , therefore the same properties than for T^+ hold.

Channel Ex: $B^0 \rightarrow a_0^+$	Contributing T & P Amplitudes	a_0		a_0					
		O	U	O	U	O	U	O	U
$B^0 \rightarrow a_0^+$	$e^i T^+ + P^+$	3_t	5	3_t	5	3_t	5	3_t	5
$\overline{B^0} \rightarrow a_0^+$	$e^{+i} T^+ + P^+$		4		4		4		-
$B^0 \rightarrow a_0^+$	$e^i T^+ + P^+$	3_t	-	3_t	-	3_t	-	-	-
$\overline{B^0} \rightarrow a_0^+$	$e^{+i} T^+ + P^+$								
Overall norm. & phase		1	2	1	2	1	2	1	2
SCCFT ($T^+ = 0$)		1	2	1	2				
Total using only B^0 's		4 vs 5		4 vs 5		5 vs 7		2 vs 3	
$B^0 \rightarrow a_0^0$	$e^i T^{00} + P^{00}$	1_i	4	3_t	4	3_t	4	1_i	4
$\overline{B^0} \rightarrow a_0^0$	$e^{+i} T^{00} + P^{00}$	1_i	-		-	3_t	-	1_i	-
Isospin relation (15)			2		2		2		2
Total adding neutral B decays		6 vs 7		7 vs 7		8 vs 9		4 vs 5	
$B^+ \rightarrow a_0^+ 0$	$e^i T^{+0} + P^{+0}$	1_i	4	1_i	4	1_i	4	1_i	4
$B^+ \rightarrow a_0^+ +$	$e^i T^{0+} + P^{0+}$	1_i	4	1_i	4	1_i	4	-	-
$B^- \rightarrow a_0^- 0$	$e^{+i} T^{+0} + P^{+0}$	1_i	-	1_i	-	1_i	-	1_i	-
$B^- \rightarrow a_0^- +$	$e^{+i} T^{0+} + P^{0+}$	1_i		1_i		1_i		-	-
Isospin relations (16)-(17)			6		6		6		4
Total adding charged B's		10 vs 9		11 vs 9		12 vs 11		6 vs 5	

Table 1: Number of observables (O) and unknowns (U) involved in the $B^0 \rightarrow a_0^+$ and $\overline{B^0} \rightarrow a_0^+$ analyses compared to the $B^+ \rightarrow a_0^+$ and $B^- \rightarrow a_0^-$ analyses. Upper part: charged final states of neutral B decays. Middle part: neutral final states of neutral B decays. Lower part: charged B decays. The time-dependence of neutral B decays yields three observables (See Eq. (14)) indicated with a ' t ' subscript, whereas the ' i ' subscript corresponds to time-integrated measurements (yielding a single observable). The fact that one can exchange the two pions in the $B^0 \rightarrow a_0^+$ final state removes half of the contribution to the number of observables and unknowns. An overall normalization and phase are subtracted from the number of unknowns, and a normalization is subtracted from the number of observables. The SCCFT argument applies to the $B^0 \rightarrow a_0^+$ and $\overline{B^0} \rightarrow a_0^+$ channels, removing one observable (because two of them turn out to measure the same quantity) and two unknowns. The number of constraints coming from isospin relations is given when available. The total number of observables vs unknowns is indicated with bold characters when the t is constrained.

whereas the $B^+ \rightarrow a_0^+$ two-body analysis consists of an eleven-parameter with one extra constraint, in the $B^+ \rightarrow a_0^+$ analysis, SCCFT decreases the number of parameters to nine, with one extra constraint. In the case where factorization does not hold for $B^- \rightarrow a_0^-$, one is left with an eleven-parameter with no extra constraints. As a consequence, SCCFT makes the $B^- \rightarrow a_0^-$ analysis more robust. The $B^- \rightarrow a_0^-$ analysis invokes a nine-parameter with two extra constraints, and finally, being a CP eigenstate, the $B^- \rightarrow a_0^-$ analysis is the simplest and is performed via a five-parameter fit.

Similarly to the $B^+ \rightarrow a_0^+$ analysis, the requirement to measure the $B^0 \rightarrow a_0^0$ branching ratio makes the $B^0 \rightarrow a_0^0$ analysis more difficult.

3.5 Mirror Solutions

CP violation in channels which benefit from SCCFT arises from interference between tree and penguin diagrams. Consequently, one measures time-dependent terms like $\sin \theta$ and $\cos \theta$. This is different from the $B^+ \rightarrow a_0^+$

analysis where tree-tree interferences result in terms like $\sin 2\theta$ and $\cos 2\theta$.

The extraction of θ via $B^0 \rightarrow a_0^0$ is done through terms like $\sin(\theta + \phi)$ and $\sin(\theta - \phi)$, where ϕ is a strong phase difference. It thus leads to multiple mirror solutions for θ , as in the two-body analyses of $B^+ \rightarrow a_0^+$ and $B^- \rightarrow a_0^-$.

In general, the number of mirror solutions depends on the type of analysis (e.g., one solution for the time-dependent Dalitz plot approach, but eight solutions for the $B^- \rightarrow a_0^-$ isospin analysis). To overcome this difficulty, the angle θ has to be measured independently in various channels.

3.6 Possible Enhancement of Direct CP Violation

Even though direct CP violation is most frequently searched for with charged B mesons, neutral B decays can also be used to look for possible asymmetries in un-

tagged sample^f:

$$B(B^0 ! a_0^+) + B(\overline{B^0} ! a_0^+) \notin \quad (19)$$

$$B(B^0 ! a_0^- +) + B(\overline{B^0} ! a_0^- +); \quad (20)$$

as well as in the tagged sample:

$$B(\overline{B^0} ! a_0^+) \notin B(B^0 ! a_0^- +); \quad (21)$$

Indeed, the suppression of the leading tree due to SC CFT may enhance direct CP violation, provided that the remaining T^+ and P^+ are of comparable magnitude. Similarly, in the charged B decays, the interference of the remaining color-suppressed tree (T^{+0}) and the non-dominant tree (T^{0+}) with penguin contributions may enhance direct CP violating effects.

In contrast to the extraction of ϵ , the enhancement of direct CP violation in the $B ! a_0$ channel does not depend on the hypotheses made in Sec. 2 (factorization and neglecting u - and c -penguin contributions), since a failure of the latter would not re-establish the hierarchy between dominant trees and penguins. The possible enhancement of direct CP violation only stems from the absence of second class currents which is experimentally established.

4 Other charm less B decays related to SC CFT

4.1 Non-Resonant $B ! D$ decay

The non-resonant $B ! D$ decay is affected by the absence of the second-class current as well: the coupling $W ! D$ remains forbidden since the D state is always produced with a natural spin-parity. As for $B ! a_0$, this can lead to an enhancement of direct CP violation. Moreover, the non-resonant decay can contribute to the extraction of ϵ (though one has to perform the full analysis without SC CFT because of the presence of non-suppressed additional trees).

Since the spin-parities of $^0(958)$ and $^0(550)$ are identical, both $B^0 ! D^+$ and $B^0 ! D^0(958)$ decays should be considered. Contributions from channels like $B^0 ! D^0(0)$ contaminate the non-resonant signal sample, and have to be vetoed.

4.2 Pure Penguin and Pure Tree $a_0 a_0$ and $b_1 b_1$ Decays

Due to SC CFT, the decays $B^0 ! a_0 a_0$ and $B^0 ! b_1 b_1$ proceed via gluonic $b ! b$ penguins only, whereas, due to the isospin relation in Eq. (18) and the relation $P^+ = P^-$, the corresponding charged B 's solely decay via tree diagrams. Therefore, there should not be any direct CP violation in these decays, and this provides a test of factorization as described in Sec. 3.1.

^f Untagged events should enter the analysis as well.

However, since only loop-processes enter these decays, contributions from new physics could modify the previous reasoning. As an example, if new physics enters through the box-diagram mediating the $B^0 \rightarrow B^0$ mixing, or equivalently through the $a_0 a_0$ and $b_1 b_1$ penguins, then, denoting the modified mixing angle θ , one would have an additional term $\sin 2(\theta) \sin(m t)$, showing direct CP violation.

4.3 $B ! a_0$ vs $a_0 K$

As in $B ! a_0$, the measurement of the ratio of $B(B^0 ! a_0) / B(B^0 ! a_0 K)$, under some assumptions (e.g., neglecting the Cabibbo suppressed tree contribution in the $B^0 ! a_0 K$ decay), can help to estimate the ratio of tree to penguin contributions to the $B ! a_0$ decay. It also gives a handle on the charm penguin contributions.

4.4 Analysis of $B^0 ! b_1$

The b_1 resonance, with even G-parity and odd spin-parity, has the same properties leading to SC CFT as the a_0 , so that the two-body analysis for ϵ can be performed accordingly.

Since the reconstruction of the b_1 proceeds through the decays $b_1 ! ! 3^0$, the higher multiplicity of the final state and the lower energy of the 3^0 renders this mode less accessible. In addition, feedthru from $W ! !$ from the $J^P = 1$ channel contaminates the $b_1(!)$ signal. On the other hand, the narrow b_1 and $! b_1$ resonances and the helicity distribution improve the background suppression.

Finally, the non-resonant $W ! !$ transition can be produced in a G-parity allowed state due to the spin 1 of the $! b_1$. Therefore, direct CP searches in the non-resonant $B ! !$ do not benefit from the absence of second class currents.

4.5 Measuring ϵ with $a_0 b_1$

Similarly to the final states, $a_0 a_0$ and $b_1 b_1$, the non-CP eigenstates $a_0 b_1$ proceed only through penguins, but the isospin suppression of the penguin contribution to the charged B decays does not apply anymore. Therefore, in contrast to the $a_0 a_0$ and $b_1 b_1$ channels, the number of observables (seven observables vs seven unknowns) is barely sufficient for the determination of ϵ .

Moreover, tests of the factorization assumption can be performed by measuring the rates of $B^0 ! a_0^+ b_1$, $B^0 ! a_0^- b_1^+$, $\overline{B^0} ! a_0^+ b_1$ and $\overline{B^0} ! a_0^- b_1^+$, which are equal if factorization holds.

Finally, the time-dependent analysis of $B^0 ! a_0 b_1$ allows the extraction of the strong phases difference between the two penguin amplitudes P^+ and P^- .

Nevertheless, since the $B \rightarrow a_0 b_1$ decay has one and four charged final state, the extraction of the signal is marred by large combinatorial background.

4.6 Decays into Higher Spin Mesons

Due to angular momentum conservation, there is no coupling of virtual W to the hadronic states of spin larger than one. The corresponding tree diagrams do not contribute to the decay amplitude thus causing effects similar to those created by SCCFT.

One example of such decays is $B^0 \rightarrow a_2(1320)$!

Other higher resonance excitations could be considered for similar analyses to those described in this article.

5 Conclusion

Constraints imposed by the absence of second class currents provide new opportunities for CP violation studies in charmless B decays. In this article, we discussed how the CKM angle can be extracted from analyses of B decays into the final states a_0 () in a more robust fashion than in the original isospin-pentagon analyses proposed for $B \rightarrow a_0$ and $B \rightarrow a_0$. A similar analysis can be performed for the decays b_1 , $a_0 b_1$ and $(^0)$, but these latter modes are experimentally much more challenging. Fits with four (if one theoretical amplitude or one ratio of amplitudes is added) to nine (with no such theoretical input) parameters can be performed for each of these decays. At combining many channels would reduce the number of mirror solutions, and decrease the error on .

Significant enhancement of direct CP asymmetries could arise in the following channels: $B \rightarrow a_0$, $B \rightarrow b_1$ and non-resonant $B \rightarrow (^0)$ due to the absence of second class currents, independently of the hypotheses needed for the extraction of (i.e., factorization and the neglect of u - and c -penguins).

Finally, many of these decays can be used to test the factorization assumption, the size of the u - and c -penguin contributions, and may be sensitive to new physics due to enhanced sensitivity to the penguin contributions.

Acknowledgments

We are indebted to Roy Aleksan, Robert Cahn, Jerome Charles, Andreas Hocker and Francois Le Diberder for their contributions to this work, and for the fruitful and cheerful collaboration.

This work was supported by the Lawrence Berkeley National Laboratory, USA, and the Laboratoire de l'Accélérateur Linéaire, France.

1. A E . Snyder, H R . Quinn, Phys.Rev.D 48 (1993) 2139

2. M . Gronau and D . London, Phys.Rev.Lett. 65 (1990) 3381
3. H J. Lipkin, Y . Nir, H R . Quinn, A E . Snyder, Phys.Rev.D 44 (1991) 1454
4. A S. Dighe, C S. Kim , Phys.Rev.D 62 (2000) 111302
5. A . Lyon for the CLEO collaboration, 'CP Violation Studies with Rare B Physics at CLEO ', talk given at BCP4, Ise-Shima, Japan, Feb.19-23, 2001
6. T J.Cham pion for the BABAR collaboration, to be published in the proceedings of 30th International Conference on High-Energy Physics (ICHEP 2000), O saka, Japan, 27 Jul - 2 Aug 2000. SLAC-PUB-8696, BABAR-PROC-00-13, hep-ex/0011018.
7. S.Versille, La violation de CP dans BaBar: etiquetage des mesons B et etude du canal $B \rightarrow a_0$, PhD thesis (in French), Universite de Paris Sud (1999)
8. Particle Data Group, C Caso et al, Eur.Phys.J C 3 (2000) 1
9. BABAR Collaboration, The BABAR Physics Book (1998)